Inorganic Chemistry
Article

Inorg. Chem. **2010**, *49*, 4507–4517 **4507**
DOI: 10.1021/ic902281a

Cyclometalated Platinum(II) 6-Phenyl-4-(9,9-dihexylfluoren-2-yl)-2,2′-bipyridine Complexes: Synthesis, Photophysics, and Nonlinear Absorption

Pin Shao,[†] Yunjing Li,[†] Jing Yi,[†] Timothy M. Pritchett,[‡] and Wenfang Sun*[,†]

[†]*Department of Chemistry and Molecular Biology, North Dakota State University, Fargo, North Dakota 58108-6050, and* [‡]*U.S. Army Research Laboratory, AMSRD-ARL-SE-EM, 2800 Powder Mill Road, Adelphi, Maryland 20783-1197*

Received November 17, 2009

A series of mononuclear and dinuclear cyclometalated platinum(II) 6-phenyl-4-(9,9-dihexylfluoren-2-yl)-2,2′-bipyridine complexes (**F-1**−**F-5**) were synthesized and their photophysical properties were systematically investigated. All complexes exhibit strong $^1\pi,\pi^*$ absorption bands in the UV region, and a broad, structureless charge transfer band in the visible region. The charge-transfer band is broadened and red-shifted for **F-3**−**F-5** compared to those for **F-1** and **F-2** because of the electron-donating acetylide ligand and the involvement of the ligand-to-ligand charge transfer character. The molar extinction coefficients for the dinuclear complex **F-5** are much higher than those for the mononuclear complexes **F-1**−**F-4**, indicating the electronic coupling through the bridge ligand. All complexes are emissive in solution at room temperature and in glassy matrix at 77 K. When excited at the charge transfer absorption band, the complexes exhibit a long-lived red/orange emission around 600 nm, which is attributed to a triplet metal-to-ligand charge transfer/intraligand charge transfer emission (^{3}MLCT/^{3}ILCT). For emission at 77 K, the emitting state is tentatively assigned as ^{3}MLCT for **F-2**−**F-4**, and ^{3}MLCT/$^3\pi,\pi^*$ for **F-1** and **F-5** taking into account the emission energy, the shape of the spectrum, the lifetime, and the thermally induced Stokes shift. **F-1**−**F-4** exhibit broad triplet transient difference absorption in the visible to the near-IR region, with a lifetime comparable to those measured from the decay of the ^{3}MLCT/^{3}ILCT emission. Therefore, **F-1**−**F-4** give rise to a strong reverse saturable absorption for ns laser pulses at 532 nm. Z-scan experiments were carried out at 532 nm using both ns and ps laser pulses, and the experimental data was fitted by a five-band model to extract the singlet and triplet excited-state absorption cross sections. The degree of reverse saturable absorption follows this trend: **F-1** = **F-2** > **F-3** > **F-4** > **F-5**, which is mainly determined by the ratio of the triplet excited-state absorption cross-section to that of the ground-state and the triplet excited-state quantum yield. Comparison of the photophysics of **F-1**, **F-2**, and **F-3** to those of their corresponding Pt complexes without the fluorenyl substituent discovers that **F-1**−**F-3** exhibit larger molar extinction coefficients for their low-energy charge transfer absorption band, longer triplet excited-state lifetimes, higher emission quantum yields, and increased ratios of the excited-state absorption cross-section to that of the ground-state.

Introduction

Square-planar platinum terdentate complexes have drawn great attention in the past two decades because of their versatile spectroscopic properties. Many of these complexes exhibit moderate charge-transfer absorption in the visible region and long-lived emission at room temperature in solution. The charge-transfer absorption band and the emission characteristics of these complexes can be readily tuned by structural modification of the ligands to meet the different requirements for diverse applications.[1,2] To date, there have been a large number of reports on the potential use of platinum terdentate complexes in light emitting diodes,[1,3] photovoltaic cells,[4] chemosensors,[5] and light modulation via nonlinear absorption.[6]

*To whom correspondence should be addressed. E-mail: wenfang.sun@ndsu.edu. Phone: 701-231-6254.

(1) Lu, W.; Mi, B. X.; Chan, M. C. W.; Hui, Z.; Che, C. M.; Zhu, N.; Lee, S. T. *J. Am. Chem. Soc.* **2004**, *126*, 4958.

(2) (a) Hua, F.; Kinayyigit, S.; Cable, J. R.; Castellano, F. N. *Inorg. Chem.* **2006**, *45*, 4304. (b) Paw, W.; Cummings, S. D.; Mansour, M. A.; Cennick, W. B.; Geiger, D. K.; Eisenberg, R. *Coord. Chem. Rev.* **1998**, *171*, 125. (c) Thomas, S. W., III; Venkatesan, K.; Müller, P.; Swager, T. M. *J. Am. Chem. Soc.* **2006**, *128*, 16641.

(3) (a) Yesin, H.; Donges, D.; Humbs, W.; Strasser, J.; Sitters, R.; Glasbeek, M. *Inorg. Chem.* **2002**, *41*, 4915. (b) Brooks, J.; Babayan, Y.; Lamansky, S.; Djurovich, P. I.; Tsyba, I.; Bau, R.; Thompson, M. E. *Inorg. Chem.* **2002**, *41*, 3055. (c) Shi, J. C.; Chao, H. Y.; Fu, W. F.; Peng, S. M.; Che, C. M. *J. Chem. Soc., Dalton Trans.* **2000**, *18*, 3128. (d) Chassot, L.; von Zelewsky, A.; Sandrini, D.; Maestri, M.; Balzani, V. *J. Am. Chem. Soc.* **1986**, *108*, 6084. (e) Maestri, M.; Sandrini, D.; Balzani, V.; Chassot, L.; Jolliet, P.; von Zelewsky, A. *Chem. Phys. Lett.* **1985**, *122*, 375. (f) Wong, W.-Y.; He, Z.; So, S.-K.; Tong, K.-L.; Lin, Z. *Organometallics* **2005**, *24*, 4079. (g) Kui, S. C. F.; Sham, I. H. T.; Cheung, C. C. C.; Ma, C.-W.; Yan, B.; Zhu, N.; Che, C.-M.; Fu, W.-F. *Chem.—Eur. J.* **2007**, *13*, 417.

© 2010 American Chemical Society
Published on Web 04/20/2010

Among the square-planar platinum complexes reported, (C^N^N)PtX complexes (C^N^N denotes 6-phenyl-2,2′-bipyridyl, X = Cl, PPh_3, acetylide, etc.)[1,3g,6c,d,7,8] are particularly interesting because of their relatively intense emission. The stronger emission from these complexes with respect to their corresponding platinum terpyridyl complexes is partially attributed to the less-distorted square-planar geometry that reduces the radiationless decay. On the other hand, because of the extended π system and the stronger σ-donating ability of the deprotonated carbon donor on the 6-phenyl ring, the energy gap between the metal-to-ligand charge transfer (MLCT) excited state and the nonemissive metal-centered d,d state is increased, which would enhance the radiative decay from the MLCT state. The better π-donating ability of the 6-phenyl ring could also introduce some intraligand charge transfer character into the emitting state,[8a] which would enhance the emission as well. Moreover, the easier structural modification of the C^N^N ligands favors the tuning of the photophysical properties of the complexes. We have demonstrated that introducing an electron-donating alkoxyl substituent on the 6-phenyl ring of the C^N^N ligand significantly increases the emission lifetime and emission efficiency through the admixture of intraligand charge transfer (ILCT) and π,π* characters into the emitting excited state.[9] In addition to the improved emission of the (C^N^N)PtX complexes, (C^N^N)PtC≡CPh and (C^N^N)-PtC_5H_7 have been demonstrated to exhibit broader triplet excited-state absorption, higher triplet excited-state quantum yield, and thus enhanced reverse saturable absorption for ns laser pulses compared to their platinum terpyridyl analogues.[6a,d] Therefore, 6-phenyl-2,2′-bipyridyl ligand is considered as a better terdentate ligand for nonlinear absorption applications. One more advantage for using the 6-phenyl-2,2′-bipyridyl ligand over the terpyridyl ligand for platinum complexation is that it will form neutral platinum chloride or acetylide complexes to increase the solubility of the complexes in common organic solvents, such as CH_2Cl_2 and CH_3CN, and therefore facilitate the purification of the platinum products.

Fluorene and its derivatives have been widely studied as building blocks for photoluminescent and electroluminescent materials[10] and two-photon absorbing materials[11] because of their rigid conjugated structures and excellent thermal and photochemical stabilities.[11] In addition, the facile substitution at the 9-position of the fluorene unit allows for easy control of the materials' properties such as solubility, processability, and morphology. Because of the aforementioned advantageous properties and the π-donating ability of fluorene, we intend to incorporate the 9,9-dihexylfluorene unit to the 4-position of the central pyridine ring of the C^N^N ligand to improve the solubility of the platinum complexes and increase the excited-state lifetime. More importantly, by introducing the fluorene unit to the platinum complexes, we expect to enhance the two-photon absorption (TPA) cross sections of the platinum complexes in the near-IR region to populate the excited state via TPA and then utilize the broad and relatively strong excited-state absorption in this region for photonic devices application.

In this work, two new C^N^N ligands containing the fluorene unit at the 4-position of the central pyridine ring and their platinum complexes with different monodentate co-ligands were synthesized and characterized. Structures of these complexes and their synthetic routes are displayed in Scheme 1. The photophysics of these complexes and their reverse saturable absorption for ns laser pulses at 532 nm were systematically investigated and analyzed.

Experimental Section

Synthesis. The compounds pyridacylpyridinium iodide,[12] **1**−**2**,[13] **3**,[14] **6**[9] and **9**−**12**[15] were prepared according to the literature procedures. All the solvents and reagents were purchased from Alfa Aesar and used as received unless otherwise stated. Column chromatography was carried out on silica gel (Sorbent Technologies, 60 Å, 230 × 450 mesh) or neutral aluminum oxide (Sigma-Aldrich, 58 Å, ∼150 mesh).

^{1}H NMR spectra were measured on a Varian 300 or 400 MHz VNMR spectrometer. High-resolution mass spectrometry was carried out on a Bruker BioTOF III mass spectrometer. Elemental analyses were carried out by NuMega Resonance Laboratories, Inc. in San Diego, California.

4. To a mixture of **3** (1.43 g, 4 mmol) and 2-acetylpyridine (0.48 g, 4 mmol) in 20 mL of ethanol, 4 mL of 1.5 M aqueous NaOH solution was added. After stirring at room temperature for 4 h, the solid formed was collected by filtration. The crude product was purified by recrystallization from methanol to afford 0.21 g yellow solid as the pure product (yield: 11%).

(4) (a) Wadas, T. J.; Chakraborty, S.; Lachicotte, R. J.; Wang, Q.-M.; Eisenberg, R. *Inorg. Chem.* **2005**, *44*, 2628. (b) Chakraborty, S.; Wadas, T. J.; Hester, H.; Flaschenreim, C.; Schmehl, R.; Eisenberg, R. *Inorg. Chem.* **2005**, *44*, 6865.

(5) (a) Yang, Q.-Z.; Wu, L.-Z.; Zhang, H.; Chen, B.; Wu, Z.-X.; Zhang, L.-P.; Tung, Z.-H. *Inorg. Chem.* **2004**, *43*, 5195. (b) Wu, L. Z.; Cheung, T. C.; Che, C. M.; Cheung, K. K.; Lam, M. H. W. *Chem. Commun.* **1998**, *10*, 1127. (c) Wong, K.-H.; Chan, M. C.-W.; Che, C. M. *Chem.—Eur. J.* **1999**, *5*, 2845. (d) Kui, S. C. F.; Chui, S. S.-Y.; Che, C.-M.; Zhu, N. *J. Am. Chem. Soc.* **2006**, *128*, 8297. (e) Wong, K. M.-C.; Tang, W.-S.; Lu, X.-X.; Zhu, N.; Yam, V. W.-W. *Inorg. Chem.* **2005**, *44*, 1492. (f) Du, P.; Schneider, J.; Brennessel, W. W.; Eisenberg, R. *Inorg. Chem.* **2008**, *47*, 69.

(6) (a) Sun, W.; Wu, Z.; Yang, Q.; Wu, L.; Tung, C. *Appl. Phys. Lett.* **2003**, *82*, 850. (b) Guo, F.; Sun, W.; Liu, Y.; Schanze, K. *Inorg. Chem.* **2005**, *44*, 4055. (c) Sun, W.; Zhu, H.; Barron, P. M. *Chem. Mater.* **2006**, *18*, 2602. (d) Shao, P.; Li, Y.; Sun, W. *J. Phys. Chem. A* **2008**, *112*, 1172. (e) Zhou, G.-J.; Wong, W.-Y.; Cui, D.; Ye, C. *Chem. Mater.* **2005**, *17*, 5209. (f) Guo, F.; Sun, W. *J. Phys. Chem. B* **2006**, *110*(30), 15029. (g) Pritchett, T. M.; Sun, W.; Guo, F.; Zhang, B.; Ferry, M. J.; Rogers-Haley, J. E.; Shensky, W., III; Mott, A. G. *Opt. Lett.* **2008**, *33*(10), 1053. (h) Shao, P.; Li, Y.; Sun, W. *Organometallics* **2008**, *27*, 2743. (i) Ji, Z.; Li, Y.; Sun, W. *Inorg. Chem.* **2008**, *47*, 7599.

(7) Cheung, T.-Z.; Cheung, K.-K.; Peng, S.-M.; Che, C.-M. *J. Chem. Soc., Dalton Trans.* **1996**, 1645.

(8) (a) Lu, W.; Chan, M. C. W.; Zhu, N.; Che, C.-M.; Li, C.; Hui, Z. *J. Am. Chem. Soc.* **2004**, *126*, 7639. (b) Shao, P.; Sun, W. *Inorg. Chem.* **2007**, *46*, 8603.

(9) Shao, P.; Li, Y.; Azenkeng, A.; Hoffmann, M.; Sun, W. *Inorg. Chem.*. **2009**, *48*, 2407.

(10) (a) Liu, B.; Bazan, G. C. *Chem. Mater.* **2004**, *16*, 4467. (b) Wang, S.; Gaylord, B. S.; Bazan, G. C. *J. Am. Chem. Soc.* **2004**, *126*, 5446. (c) Scherf, U.; List, E. J. M. *Adv. Mater.* **2002**, *14*, 477. (d) Setayesh, S.; Grimsdale, A. C.; Weil, T.; Enkelmann, V.; Müllen, K.; Meghdadi, F.; List, E. J. W.; Leising, G. *J. Am. Chem. Soc.* **2001**, *123*, 946. (e) Ostrowski, J. C.; Robinson, M. R.; Heeger, A. J.; Bazan, G. C. *Chem. Common.* **2002**, 784.

(11) (a) Reinhardt, B. A.; Brott, L. L.; Clarson, S. J.; Dillard, A. G.; Bhatt, J. C.; Kannan, R.; Yuan, L.; He, G. S.; Prasad, P. N. *Chem. Mater.* **1998**, *10*, 1863. (b) Belfield, K. D.; Hagan, D. J.; Van Stryland, E. W.; Schafer, K. J.; Negres, R. A. *Org. Lett.* **1999**, *1*, 1575. (c) Werts, M. H. V.; Gmouh, S.; Mongin, O.; Pons, T.; Blanchard-Desce, M. *J. Am. Chem. Soc.* **2004**, *126*, 16294. (d) Day, P. N.; Nguyen, K. A.; Pachter, R. *J. Phys. Chem. B* **2005**, *109*, 1803.

(12) Neve, F.; Crispini, A.; Campagna, S.; Serroni, S. *Inorg. Chem.* **1999**, *38*, 2250.

(13) Koizumi, Y.; Seki, S.; Tsukuda, S.; Sakamoto, S.; Tagawa, S. *J. Am. Chem. Soc.* **2006**, *128*, 9036.

(14) He, F.; Xia, H.; Tang, S.; Duan, Y.; Zeng, M.; Liu, L.; Li, M.; Zhang, H.; Yang, B.; Ma, Y.; Liu, S.; Shen, J. *J. Mater. Chem.* **2004**, *14*, 2735.

(15) Lee, S. H.; Nakamura, T.; Tsutsui, T. *Org. Lett.* **2001**, *3*, 2005.

Scheme 1. Synthetic Routes for Complexes **F-1**−**F-5**

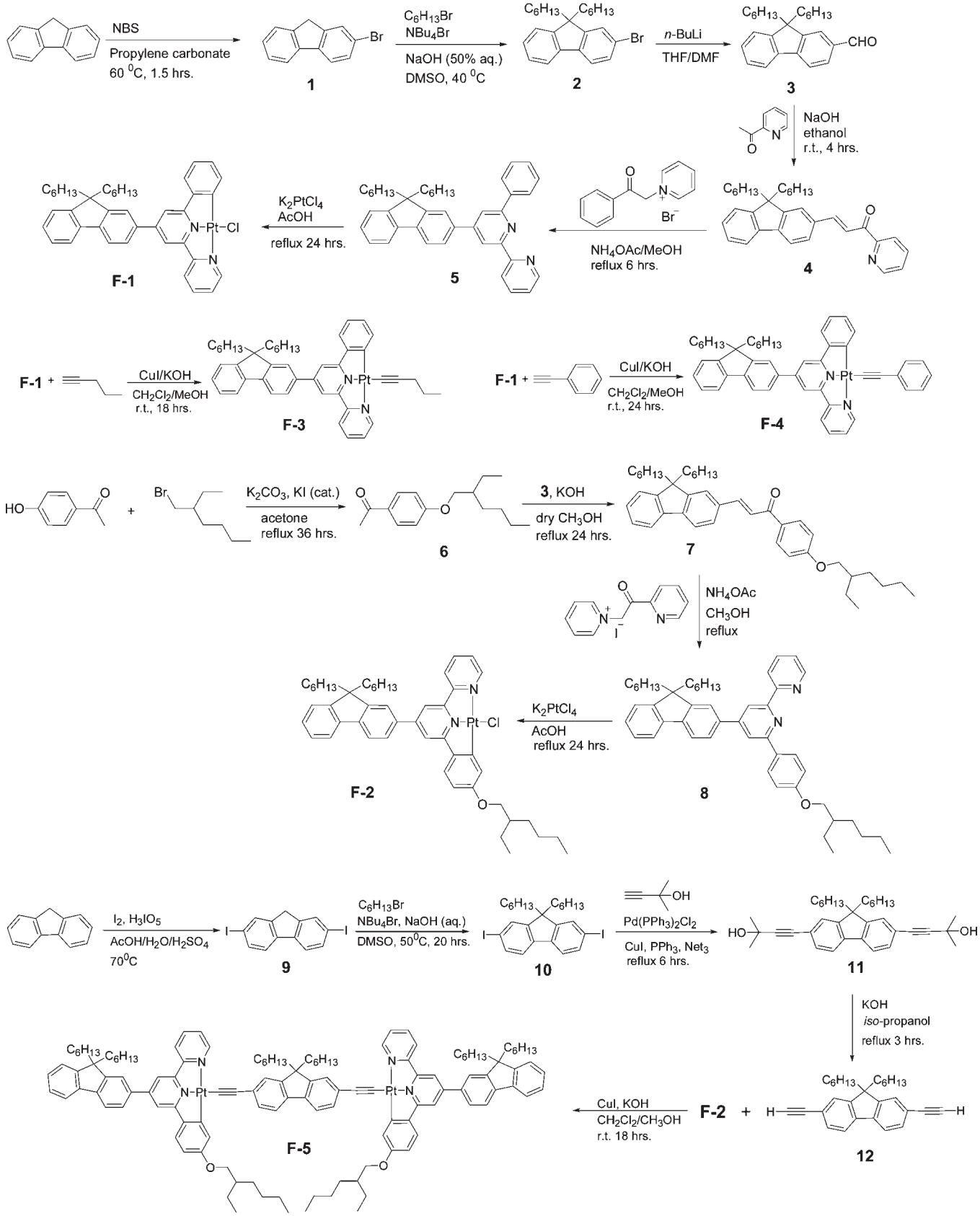

^{1}H NMR ($CDCl_3$): δ 8.79 (d, J = 4.5 Hz, 1H), 8.32 (d, J = 16.2 Hz, 1H), 8.23 (d, J = 8.1 Hz, 1H), 8.06 (d, J = 16.2 Hz, 1H), 7.88−7.93 (m, 1H), 7.72 (d, J = 5.1 Hz, 4H), 7.50−7.54 (m, 1H), 7.35 (d, J = 3.3 Hz, 3H), 1.98−2.04 (m, 4H), 1.04−1.14 (m, 12H), 0.75 (t, J = 6.6 Hz, 6H), 0.59−0.63 (m, 4H) ppm. ESI-HRMS: m/z calcd for $[C_{33}H_{39}NO+H]^+$: 466.3104; found, 466.3124. Anal. Calcd (%) for $C_{33}H_{39}NO$: C, 85.11; H, 8.44; N 3.01. Found: C, 84.75; H, 8.90; N, 3.05.

5. A mixture of **4** (1.42 g, 3 mmol), *N*-(benzoylmethyl)-pyridinium bromide (0.85 g, 3 mmol) and NH_4OAc (3.00 g, 39 mmol) in 70 mL of methanol was refluxed for 6 h. Methanol was removed and 40 mL of water was added to the residue. The resultant mixture was extracted with CH_2Cl_2. The organic layer was washed with brine (40 mL×2) and dried over Na_2SO_4. The crude product was purified using a silica gel column eluted with hexane/ethyl acetate (v/v = 20:1) to yield 0.75 g of a colorless viscous oil (yield: 44%). ^{1}H NMR ($CDCl_3$): δ 8.77−8.80 (m, 1H), 8.73−8.76 (m, 2H), 8.29 (dd, J = 1.5, 8.4 Hz, 2H), 8.09 (d, J = 1.5 Hz, 1H), 7.91 (dd, J = 2.1, 7.5 Hz, 1H), 7.86−7.89 (m, 2H), 7.83 (d, J = 1.2 Hz, 1H), 7.78−7.81 (m, 1H), 7.59 (td, J = 1.5, 6.6 Hz, 2H), 7.47−7.53 (m, 1H), 7.35−7.44 (m, 4H), 2.02−2.13 (m, 4H), 1.11−1.19 (m, 12H), 0.73−0.82 (m, 10H) ppm. ESI-HRMS: m/z calcd for $[C_{41}H_{44}N_2+H]^+$: 565.3577; found, 565.3572. Anal. Calcd (%) for $C_{41}H_{44}N_2$: C, 87.19; H, 7.85; N, 4.96. Found: C, 86.91; H, 8.05; N, 4.97.

7. A mixture of **3** (1.17 g, 3.23 mmol), **6** (0.80 g, 3.23 mmol), and KOH (0.84 g, 15 mmol) in dry MeOH (80 mL) was refluxed for 24 h. The solvent was removed, and 40 mL of water was added to the residue. The resultant mixture was extracted with ether. The organic layer was washed with brine and dried over Na_2SO_4. The crude product was purified by a silica gel column eluted with CH_2Cl_2/hexane (v/v = 1:1) to afford 0.71 g of yellow oil (yield: 37%). ^{1}H NMR ($CDCl_3$): δ 8.09 (d, J = 8.4 Hz, 2H), 7.93 (d, J = 15.6 Hz, 1H), 7.71−7.73 (m, 2H), 7.59−7.66 (m, 3H), 7.34 (d, J = 2.4 Hz, 3H), 7.00 (d, J = 8.4 Hz, 2H), 3.93 (d, J = 5.4 Hz, 2H), 1.98−2.04 (m, 4H), 1.75−1.77 (m, 1H), 1.33−1.54 (m, 8H), 1.05−1.14 (m, 12H), 0.86−0.97 (m, 6H), 0.73−0.78 (m, 6H), 0.63 (s, 4H) ppm. ESI-HRMS: m/z calcd for $[C_{42}H_{56}O_2+H]^+$: 593.4353; found, 593.4363. Anal. Calcd (%) for $C_{42}H_{56}O_2 \cdot C_6H_{14}$: C, 84.89; H, 10.40. Found: C, 85.35; H, 10.70.

8. A mixture of **7** (1.46 g, 2.5 mmol), pyridacylpyridinium iodide (0.80 g, 2.5 mmol) and NH_4OAc (2.00 g, 26 mmol) was refluxed in 50 mL of MeOH for overnight. The solvent was removed, and 40 mL of ether was added to the residue. The resultant mixture was washed with brine and dried over Na_2SO_4. The crude product was purified by a silica gel column eluted with CH_2Cl_2/hexane (v/v = 1:1) to give 0.22 g of a colorless viscous oil (yield: 13%). ^{1}H NMR ($CDCl_3$): δ 8.73 (d, J = 4.8 Hz, 1H), 8.68 (d, J = 7.8 Hz, 1H), 8.61 (d, J = 1.2 Hz, 1H), 8.17 (d, J = 8.7 Hz, 2H), 7.97 (d, J = 1.2 Hz, 1H), 7.84−7.90 (m, 1H), 7.80 (t, J = 1.2 Hz, 2H), 7.73−7.76 (m, 2H), 7.32−7.37 (m, 4H), 7.05 (d, J = 9.0 Hz, 2H), 3.93 (d, J = 5.7 Hz, 2H), 2.00−2.05 (m, 4H), 1.73−1.80 (m, 1H), 1.33−1.55 (m, 8H), 1.05−1.14 (m, 12H), 0.91−0.97 (m, 6H), 0.75 (t, J = 6.3 Hz, 6H), 0.64−0.66 (m, 4H) ppm. ESI-HRMS: m/z calcd for $[C_{49}H_{60}N_2O+H]^+$: 693.4778; found, 693.4809. Anal. Calcd (%) for $C_{49}H_{60}ON_2 \cdot {}^1/_3CH_2Cl_2$: C, 82.14; H, 8.48; N, 3.88. Found: C, 82.23; H, 8.27; N, 3.56.

F-1. A mixture of ligand **5** (0.20 g, 0.35 mmol) and K_2PtCl_4 (0.15 g, 0.35 mmol) was refluxed in 60 mL of AcOH for 24 h. After being cooled to room temperature, the yellow precipitant was collected by filtration. The crude product was purified by a neutral alumina gel column eluted with CH_2Cl_2, and then further purified by recrystallization from CH_2Cl_2/ether. Orange solid was obtained as the pure product (0.23 g, yield: 83%). ^{1}H NMR ($CDCl_3$): δ 8.73 (d, J = 5.4 Hz, 1H), 7.92 (d, J = 3.6 Hz, 2H), 7.85 (d, J = 8.4 Hz, 1H), 7.78−7.81 (m, 1H), 7.72−7.74 (m, 2H), 7.60 (d, J = 1.8 Hz, 1H), 7.44 (dd, J = 7.2, 1.2 Hz, 1H), 7.37−7.41 (m, 3H), 7.31 (t, J = 4.2 Hz, 2H), 7.22−7.24 (m, 1H), 6.96 (td, J = 1.2, 7.8 Hz, 1H), 6.88 (td, J = 1.2, 7.5 Hz, 1H), 2.07−2.16 (m, 4H), 1.09−1.14 (m, 12H), 0.76 (t, J = 6.6 Hz, 6H), 0.69 (br. s, 4H) ppm. ESI-MS: m/z calcd for $[C_{41}H_{43}N_2{}^{195}Pt+CH_3CN]^+$, 799.3338; found, 799.3396. Anal. Calcd (%) for $C_{41}H_{43}ClN_2Pt$: C, 61.99; H, 5.46; N, 3.53. Found: C, 62.30; H, 5.10; N, 3.64.

F-2. A mixture of **8** (0.25 g, 0.36 mmol) and K_2PtCl_4 (0.15 g, 0.36 mmol) was refluxed in 60 mL of AcOH for 24 h. After being cooled down to room temperature, the solid formed was collected by filtration. The crude product was purified by a neutral alumina gel column eluted by CH_2Cl_2, and then recrystallized from CH_2Cl_2/hexane. A 0.25 g portion of orange solid was obtained as the pure product (yield: 76%). ^{1}H NMR ($CDCl_3$): δ 8.72 (d, J = 5.1 Hz, 1H), 7.77−7.82 (m, 5H), 7.71 (d, J = 8.1 Hz, 1H), 7.46 (s, 1H), 7.36−7.39 (m, 3H), 7.18−7.23 (m, 2H), 7.15 (d, J = 8.4 Hz, 1H), 6.98 (d, J = 2.4 Hz, 1H), 6.49 (d, J = 8.4 Hz, 1H), 3.72 (d, J = 5.7 Hz, 2H), 2.06−2.12 (m, 4H), 1.67−1.72 (m, 1H), 1.26−1.51 (m, 8H), 1.05−1.15 (m, 12H), 0.85−0.90 (m, 6H), 0.72−0.79 (m, 10H) ppm. ESI-MS: m/z calcd for $[C_{49}H_{59}N_2O{}^{195}Pt+CH_3CN]^+$, 927.4539; found, 927.4551. Anal. Calcd (%) for $C_{49}H_{59}ClN_2OPt$: C, 63.79; H, 6.45; N, 3.04. Found: C, 63.82; H, 6.22; N, 3.35.

F-3. A mixture of **F-1** (0.13 g, 0.16 mmol), 1-pentyne (40 μL, 0.41 mmol), CuI (3.0 mg, 0.01 mmol), and KOH (60 mg, 1 mmol) in degassed CH_2Cl_2/CH_3OH (40 mL/20 mL) was stirred at room temperature under argon for 18 h. After the reaction, the solvent was removed, and the crude product was purified by a neutral alumina gel column eluted by CH_2Cl_2/hexane (v/v = 3:1), and then recrystallized from CH_3OH. Red solid was obtained as the pure product (89 mg, yield: 67%). ^{1}H NMR ($CDCl_3$): δ 9.05 (d, J = 5.4 Hz, 1H), 7.92−7.98 (m, 2H), 7.69−7.86 (m, 5H), 7.60 (s, 1H), 7.53 (s, 1H), 7.34−7.38 (m, 5H), 6.96−7.05 (m, 2H), 2.68 (t, J = 7.2 Hz, 2H), 2.02−2.08 (m, 4H), 1.67−1.77 (m, 2H), 1.07−1.17 (m, 15H), 0.67−0.77 (m, 10H) ppm. ESI-MS: m/z calcd for $[C_{46}H_{50}N_2{}^{195}Pt+H]^+$, 826.3698; found, 826.3695. Anal. Calcd (%) for $C_{46}H_{50}N_2Pt$: C, 66.89; H, 6.10; N, 3.39. Found: C, 66.51; H, 6.37; N, 3.54.

F-4. A mixture of **F-1** (0.13 g, 0.16 mmol), phenylacetylene (24 μL, 0.24 mmol), CuI (3.0 mg, 0.01 mmol), and KOH (60 mg, 1.00 mmol) in degassed CH_2Cl_2/CH_3OH (50 mL/25 mL) was stirred at room temperature under argon for 24 h. The solvent was removed, and the crude product was purified by a neutral alumina gel column with CH_2Cl_2/hexane (v/v = 3:1) used as the eluent. Recrystallization from CH_2Cl_2/ether yields 82 mg of a red solid as the pure product (yield: 59%). ^{1}H NMR ($CDCl_3$): δ 9.10 (d, J = 4.8 Hz, 1H), 8.01 (d, J = 4.4 Hz, 2H), 7.75−7.81 (m, 4H), 7.71 (d, J = 8.0 Hz, 1H), 7.64 (s, 1H), 7.58 (d, J = 8.0 Hz, 3H), 7.37−7.43 (m, 6H), 7.29 (t, J = 8.0 Hz, 2H), 7.18−7.20 (m, 1H), 7.03 (dd, J = 3.2, 5.6 Hz, 1H), 2.01−2.05 (m, 4H), 1.07−1.14 (m, 12H), 0.76 (t, J = 7.2 Hz, 6H), 0.66 (br. s, 4H) ppm. ESI-MS: m/z calcd for $[C_{49}H_{48}N_2{}^{195}Pt+Na]^+$, 882.3362; found, 882.3343. Anal. Calcd (%) for $C_{49}H_{48}N_2Pt \cdot 0.1CH_2Cl_2$: C, 67.90; H, 5.59; N, 3.23. Found: C, 67.70; H, 5.26; N, 3.38.

F-5. A mixture of **F-2** (0.48 g, 0.52 mmol), **12** (0.10 g, 0.26 mmol), CuI (6.0 mg, 0.02 mmol), and KOH (56 mg, 1.0 mmol) in degassed CH_2Cl_2/CH_3OH (50 mL/40 mL) was stirred at room temperature under argon for 18 h. The solvent was removed, and the crude product was purified by a neutral alumina gel column (CH_2Cl_2/hexane (v/v = 3:1) was used as the eluent), and then recrystallized from CH_2Cl_2/ether. Red solid was obtained as the pure product (0.34 g, yield: 30%). ^{1}H NMR ($CDCl_3$): δ 9.38 (d, J = 5.7 Hz, 2H), 8.05 (s, 4H), 7.57−7.82 (m, 22H), 7.45 (d, J = 8.4 Hz, 2H), 7.39 (br. s, 6H), 6.65 (d, J = 9.0 Hz, 2H), 4.03 (br. s, 4H), 2.02 (br. s, 12H), 1.78 (br. s, 2H), 1.35−1.52 (m, 16H), 1.08−1.23 (m, 36H), 0.91−0.98 (m, 12H), 0.75−0.78 (m, 30H) ppm. ESI-MS: m/z calcd for $[C_{127}H_{150}N_4O_2Pt_2+2Na]^{2+}$, 1100.0432; found, 1100.0466. Anal. Calcd (%) for $C_{127}H_{150}N_4O_2Pt_2$: C, 70.79; H, 7.02; N, 2.60. Found: C, 70.73; H, 6.69; N, 2.64.

Photophysical Measurements. The UV−vis absorption spectra were measured using an Agilent 8453 spectrophotometer in a 1 cm or 1 mm quartz cuvette. The steady-state emission spectra were obtained on a SPEX fluorolog-3 fluorometer/phosphorometer. The emission quantum yields were determined by the optical dilute method[16] in degassed solutions, and a degassed aqueous solution of $[Ru(bpy)_3]Cl_2$ (Φ_{em} = 0.042, λ_{ex} = 436 nm)[17]

(16) Demas, J. N.; Crosby, G. A. *J. Phys. Chem.* **1971**, *75*, 991.
(17) Van Houten, J.; Watts, R. *J. Am. Chem. Soc.* **1976**, *98*, 4853.

was used as the reference. The excited-state lifetimes, the triplet excited-state quantum yields, and the triplet transient difference absorption spectra were measured in degassed solutions on an Edinburgh LP920 laser flash photolysis spectrometer. The third harmonic output (355 nm) of a Nd:YAG laser (Quantel Brilliant, pulsewidth ~4.1 ns, repetition rate was set at 1 Hz) was used as the excitation source. Each sample was purged with Ar for 30 min before measurement.

The self-quenching rate constants (k_Q) in CH_2Cl_2 were deduced followed the Stern−Volmer equation:

$$k_{obs} = k_Q[C] + k_0 \quad (1)$$

where k_{obs} is the decay rate constant of the emission ($k_{obs} = 1/\tau_{em}$), k_Q is the self-quenching rate constant, [C] is the concentration of the complex in mol/L, and k_0 ($k_0 = 1/\tau_0$) is the decay rate constant of the excited state at infinite dilute solution. A plot of the observed decay rate constant versus concentration should give rise to a straight line. The slope of the straight line corresponds to k_Q and the intercept corresponds to k_0.

The triplet excited-state molar extinction coefficient and triplet quantum yield were determined by the partial saturation method.[18] The optical density at the interested wavelength was monitored when the excitation energy at 355 nm was gradually increased. Saturation was observed when the excitation energy was higher than 10 mJ. The following equation was then used to fit the experimental data to obtain the ε_T and Φ_T.[18]

$$\Delta OD = a(1 - \exp(-bI_p)) \quad (2)$$

where ΔOD is the optical density at the interested wavelength, I_p is the pump intensity in Einstein·cm^{-2}, $a = (\varepsilon_T - \varepsilon_0)dl$, and $b = 2303\,\varepsilon_0^{ex}\Phi_T/A$. ε_T and ε_0 are the absorption coefficients of the excited state and the ground state at the interested wavelength, ε_0^{ex} is the ground state absorption coefficient at the excitation wavelength of 355 nm, d is the concentration of the sample (mol L^{-1}), l is the thickness of the sample, and A is the area of the sample irradiated by the excitation beam.

Nonlinear Transmission Measurements. The experimental setup was similar to what had been described previously,[6c] with a 20 cm focal-length lens used to focus the beam to the 2 mm thick sample cuvette.

Z-Scan Measurements. The open-aperture experimental setup is similar to the one reported previously.[19] For ns Z-scan measurements, the second harmonic output (532 nm) from a Quantel Brilliant Nd:YAG laser with a pulsewidth of 4.1 ns and a repetition rate of 10 Hz was used as the light source. The laser beam was focused by a 30 cm focal-length plano-convex lens to a beam waist of 30 μm at the focal point, which corresponds to a Rayleigh length ($z_0 = \pi\omega_0^2/\lambda$, where ω_0 is the radius at the beam waist) of 5.31 mm. For ps Z scans, the light source was the second harmonic output of an EKSPLA PL2143A passively mode-locked, Q-switched Nd:YAG laser (pulsewidth = 21 ps, repetition rate = 10 Hz). A 15 cm plano-convex lens was used to focus the beam to a beam waist of 34 μm at the focal point, which gave rise to a Rayleigh length of 6.82 mm. Therefore, the sample solution placed in a 1 mm thick quartz cuvette for ns measurements and in a 2 mm cuvette for ps measurements could be considered as thin samples. A 50 cm plano-convex lens was placed at approximately 30 cm after the linear focal plane to collect all of the transmitted light into the Molectron J4−09 joulemeter probe.

To fit the Z-scan experimental data, we used a five-band model that consists of a ground state, two singlet excited states and two triplet excited states. The detailed descriptions of the model and the fitting procedure were reported previously by our group.[19]

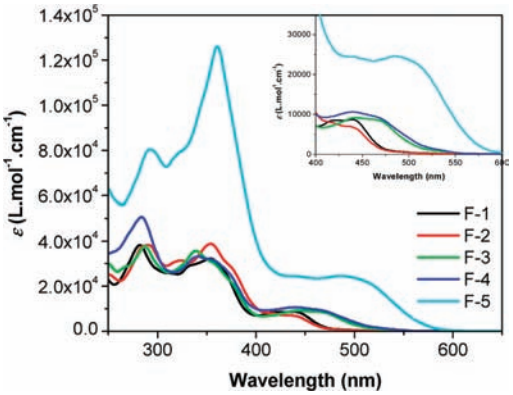

Figure 1. UV−vis absorption spectra of **F-1**−**F-5** in CH_2Cl_2. $c = 5 \times 10^{-5}$ mol/L. The inset shows the expansion of the charge transfer band.

Results and Discussion

Electronic Absorption. The UV−vis absorption spectra of **F-1**−**F-5** were investigated in CH_2Cl_2 at different concentrations (5×10^{-6} to 5×10^{-4} mol/L), and the results are presented in Figure 1 for a concentration of 5×10^{-5} mol/L. The absorption of all five complexes obeys Lambert−Beer's law in the concentration range studied, indicating that no ground-state aggregation occurs in this concentration range. The intense absorption below 400 nm for these complexes could be assigned to the intraligand π,π^* transitions within the 4-fluorenyl-C^N^N ligand because these bands are essentially independent of the monodentate co-ligand. The broad, moderately intense absorption band in the visible region, that is, 400−500 nm for **F-1** and **F-2**, 410−550 nm for **F-3** and **F-4**, and 420−600 nm for **F-5**, could be tentatively attributed to the admixture of ^{1}MLCT (metal-to-ligand charge transfer)/^{1}ILCT (intraligand charge transfer) transitions for **F-1** and **F-2**, and ^{1}MLCT/^{1}ILCT/^{1}LLCT (ligand-to-ligand charge transfer) for **F-3**−**F-5** considering the similar shape and energy of this band to those reported in the literature for other platinum C^N^N and terpyridyl acetylide complexes.[1,3g,6d,7−9,20] The involvement of the intraligand charge transfer (^{1}ILCT) character into the charge-transfer band of these complexes should be taken into account because of the π-donating ability of the fluorenyl unit on the C^N^N ligand, which is similar to that previously reported by our group for platinum C^N^N complexes with an electron-donating alkoxyl substituent on the 6-phenyl ring of the C^N^N ligand[9] and for platinum terpyridyl complexes with a dimethylamino substituent on the 4′-position of the terpyridine ligand.[21] Another piece of evidence that supports this hypothesis arises from the enhanced intensity of the charge transfer band of these complexes compared to their respective platinum C^N^N complexes without the 4-fluorenyl substituent[9] (exemplified by **F-1**−**F-3** in Supporting Information Figure S1). The charge transfer band becomes broadened and red-shifted for **F-3**− **F-5**

(18) Carmichael, I.; Hug, G. L. *J. Phys. Chem. Ref. Data* **1986**, *15*, 1.
(19) Li, Y.; Pritchett, T. M.; Huang, J.; Ke, M.; Shao, P.; Sun, W. *J. Phys. Chem. A* **2008**, *112*, 7200.
(20) Fan, Y.; Zhang, L.-Y.; Dai, F.-R.; Shi, L.-X.; Chen, Z.-N. *Inorg. Chem.* **2008**, *47*, 2811.
(21) Ji, Z.; Azenkeng, A.; Hoffmann, M.; Sun, W. *Dalton Trans.* **2009**, 7725.

comparing to those of **F-1** and **F-2**. Such a feature could be rationalized by two factors: First, the stronger π-donating ability of the acetylide in **F-3**−**F-5** could raise the Pt d orbitals, and thus decreases the energy gap between the bipyridine-based lowest unoccupied molecular orbital (LUMO)[9] and the d orbital. This would consequently decrease the energy of the ^{1}MLCT excited state. Second, the acetylide ligand would admix more LLCT character into the lowest excited state with the increased π-donating ability of the acetylide ligand, which would also cause the broadening and red-shift of the charge-transfer band.

A point worthy of addressing is the influence of the 4-fluorenyl substituent on the UV−vis absorption spectra of **F-1**−**F-5**. As shown in Supporting Information, Figure S1 for **F-1**−**F-3**, the transition energies in these complexes are quite similar to those of their corresponding platinum C^N^N complexes without the 4-fluorenyl substituent,[9] especially for the lowest-energy charge transfer bands, indicating that the fluorenyl substituent has a negligible effect on the energy level of the bipyridine based LUMO (π*(N^N)) for the Pt(C^N^N)X complexes.[9] However, the presence of the fluorenyl substituent significantly increases the molar extinction coefficients for the bands above 300 nm. This phenomenon likely arises from the extended π-system in the fluorenyl-substituted complexes, which could increase the oscillator strength for these transitions by increasing the transition dipoles.[6b]

It is also interesting to note that the extinction coefficients for the dinuclear complex **F-5** are much larger than those of the mononuclear complexes **F-1**−**F-4**. The extinction coefficients of the bands at about 360 and 490 nm are more than double of the respective bands in the mononuclear complexes, and the ε value at the low-energy absorption band apex is approximately 2.4×10^4 M^{-1} cm^{-1}, which is similar to the value of a binuclear platinum terpyridyl 1,10-phenanthrolineethynyl complex (2.2×10^4 M^{-1} cm^{-1}).[20] This indicates that interactions between the two Pt(C^N^N) components could occur through the rigid conjugated bridging ligand.

The charge transfer nature of the low-energy absorption bands in **F-1**−**F-5** is supported by the solvent-dependency studies. As exemplified in Figure 2 for **F-4**, the low-energy absorption band energy bathochromically shifts to longer wavelengths in solvents with lower polarity (such as hexane and CH_2Cl_2) compared to those in more polar solvents (i.e., CH_3CN and CH_3OH). This negative solvatochromic effect is a characteristic of a charge-transfer transition, in which the ground state is more polar than the excited state, and is in line with many of the platinum C^N^N or terpyridyl complexes reported in the literature.[1,3g,6d,7,8]

Emission. F-1−**F-5** are emissive in solutions at room temperature and in glassy solutions at 77 K. Figure 3 show the emission spectra of **F-1**−**F-5** in CH_2Cl_2 solution at a concentration of 5×10^{-5} mol/L at room temperature when excited at their respective charge transfer band. When excited at their ~350 nm π,π* transition bands, **F-1**−**F-4** give rise to the same red/orange emission band as that observed from excitation at their charge transfer bands. In contrast, **F-5** exhibits a structured emission in the 320−500 nm regions in addition to the broad structureless emission band in the 500−750 nm regions (shown in Figure 4) upon excitation at $\lambda_{ex} \leq 370$ nm. The lifetimes of these two emission bands are quite distinct. The lifetime of the high-energy band is too short to be measured on our instrument, which is expected to be shorter than 5 ns; while the lifetime of the orange emission band is hundreds of nanoseconds. In addition, the excitation spectra corresponding to these two emission bands are different. The excitation spectrum monitored at the high-energy band is consistent with the π,π* transition bands in the UV region (Supporting Information, Figure S2). In contrast, the excitation spectrum measured for the orange emission corresponds to the charge transfer band in the UV−vis absorption spectrum (Supporting Information, Figure S2). Considering the different lifetimes, the distinct excitation spectra, and the different Stokes shifts, we tentatively attribute the high-energy emission from **F-5** to fluorescence from the $^1\pi$,π* state of the 2,7-diethynyl-9,9-dihexylfluorenyl bridging ligand; whereas the red/orange emission from **F-1**−**F-5** is assigned as a triplet excited-state with charge transfer character, likely to be ^{3}MLCT/^{3}ILCT with reference to the other platinum C^N^N complexes reported in the literature.[1,3g,6d,7−9,20] The charge transfer nature of the red/orange emission band could be supported by the fact that this band exhibits a negative solvatochromic effect. As shown in Figure 5 for complex **F-4**, the emission energy decreases in less polar solvents such as hexane

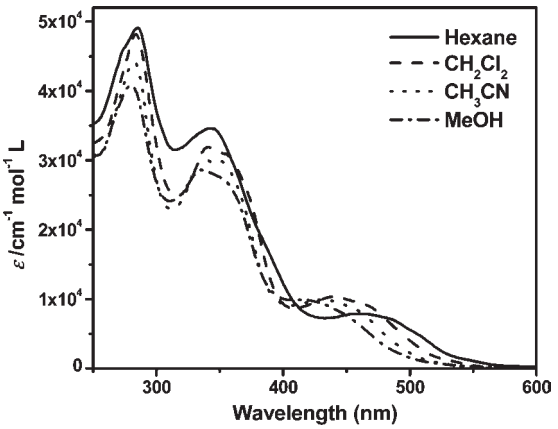

Figure 2. UV−vis absorption spectra of **F-4** in different solvents. $c = 5 \times 10^{-5}$ mol/L.

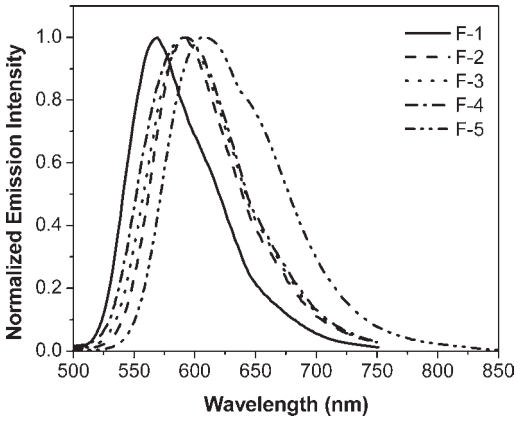

Figure 3. Normalized emission spectra of **F-1**−**F-5** in CH_2Cl_2 at a concentration of 5×10^{-5} mol/L. The excitation wavelength is 440 nm.

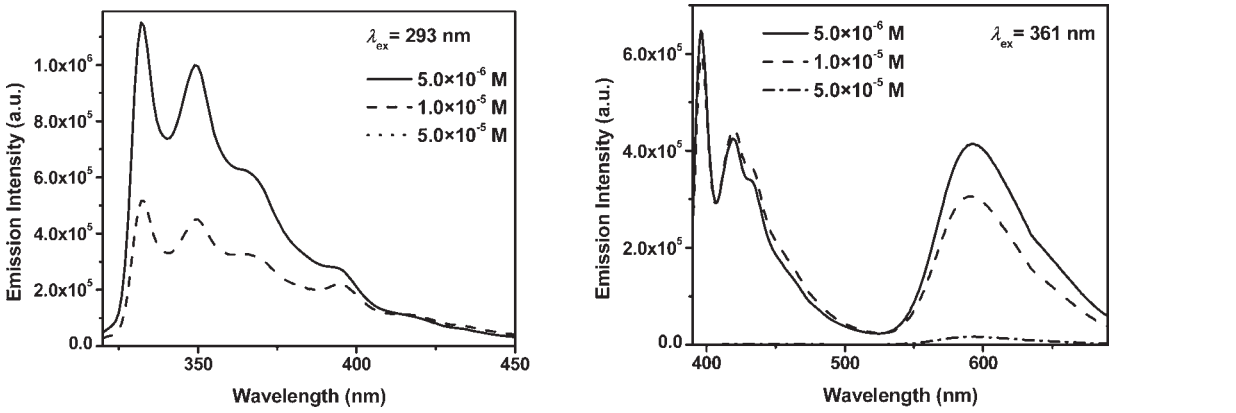

Figure 4. Emission spectra of **F-5** in CH_2Cl_2 at room temperature with different excitation wavelengths.

and toluene in comparison to those in polar solvents CH_2Cl_2 and CH_3CN. The same solvent effect was observed for the other four complexes as well.

It is important to note that the high-energy emission band observed in the solution of **F-5** cannot be attributed to a trace amount of uncoordinated 4-fluorenyl-C^N^N ligand or fluorenyl impurity because the free 4-fluorenyl-C^N^N ligand exhibits a structureless fluorescence at 378 nm in CH_2Cl_2 upon excitation at 325 nm and the free fluorene shows a slightly structured fluorescence at 312 nm in CH_2Cl_2 upon excitation at 265 nm (Supporting Information, Figure S3). Neither the emission energy nor the spectral feature from the free 4-fluorenyl-C^N^N ligand and free fluorene is consistent with the high-energy band observed in **F-5** solution. However, this high-energy fluorescence band is essentially the same as the fluorescence spectrum of 2,7-diethynyl-9,9-dihexylfluorene (Supporting Information, Figure S3(c)). The fact that this band is only observed from **F-5** solution but not from the solutions of the other four complexes also suggests that this band is associated with the unique structural feature of **F-5**, that is, the presence of the 2,7-diethynyl-9,9-dihexylfluorenyl bridging ligand. We believe that this high-energy emission band in **F-5** solution indeed emanates from the coordinated bridging ligand, rather than the free bridging ligand impurity because the excitation spectrum (Supporting Information, Figure S2(a)) giving rise to this band is quite different from that measured in the free ligand (Supporting Information, Figure S3(d)).

The possibility of the low-energy red/orange emission band arising from fluorescence resonance energy transfer (FRET) from the fluorenyl component to the Pt(C^N^N) component could be excluded based on the fact that no low-energy red/orange emission band appears in the emission spectrum of the free 4-fluorenyl-C^N^N ligand (Supporting Information, Figure S3(a)).

The concentration-dependent emission was investigated for all five complexes. When the concentration is increased from 5×10^{-6} mol/L to 5×10^{-4} mol/L, the emission energies and the shapes of the spectra of **F-1**−**F-4** remain essentially the same (exemplified in Supporting Information, Figure S4 for **F-4**); however, the emission intensity decreases at high concentrations and the emission lifetimes decrease with increased solution concentration. Because these complexes have almost no ground-state absorption at the emission band apex and the shapes

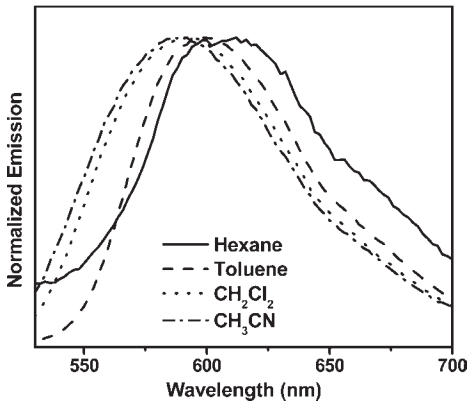

Figure 5. Emission spectra of **F-4** in different solvents at room temperature. $c = 5 \times 10^{-5}$ mol/L. $\lambda_{ex} = 440$ nm.

of the spectra are the same, self-absorption of emission could be excluded. As discussed in the previous section, the UV−vis absorption obeys the Lambert−Beer's law in the concentration range of 5×10^{-6} mol/L to 5×10^{-4} mol/L, suggesting that no ground-state aggregation occurs in this concentration range. Therefore, the intensity decrease at high concentrations cannot be attributed to the ground-state aggregation. In view of the decreased lifetime at high concentrations, it is clear that self-quenching occurs at high concentrations. The self-quenching rate constants (k_Q) were measured according to the Stern−Volmer relation, and the results are listed in Table 1. The k_Q for **F-1**−**F-4** varies between 1.12×10^9 and 1.63×10^9 L mol^{-1} s^{-1}, which falls in the same order of values reported for the terpyridine platinum phenylacetylide complexes ($1.45\times10^9-1.74\times10^9$ L mol^{-1} s^{-1}).[22] A feature worthy of mention is that the self-quenching constant for **F-1** is much higher than that for **F-2**. This could be explained by the presence of the branched alkoxyl chain in **F-2**, which could reduce the π,π stacking and thus the formation of excimer.

Complex **F-5** exhibits a slightly different concentration-dependent behavior from the other four complexes. As shown in Figure 6, the emission band maximum gradually red-shifts with increased concentration accompanied by reduced intensity and shortened lifetime. In view of the

(22) Yam, V. W.-W.; Tang, R. P.-L.; Wong, K. M.-C.; Cheung, K.-K. *Organometallics* **2001**, *20*, 4476.

Table 1. Photophysical Parameters of **F-1**−**F-5**

	CH_2Cl_2[a]			CH_3CN[a]		C_3H_7CN[b]
	λ_{abs}[c]/ nm ($\varepsilon/10^3$ L·mol^{-1}·cm^{-1})	λ_{em}[c]/nm (τ_0/ns; Φ_{em})	k_Q[d]/10^9 L·mol^{-1}·s^{-1}	λ_{em}[c]/ nm (τ_{em}/ ns, Φ_{em})	$\lambda_{T1\text{-}Tn}$/ nm (τ_{TA}/ ns; $\varepsilon_{T1\text{-}Tn}$/ L·mol^{-1}·cm^{-1}; Φ_T)	λ_{em}[c]/nm (τ_{em}/μs)
F-1	282 (38.2), 312 (25.9), 336 (29.6), 354 (32.3), 421 (8.6), 439 (8.8)	568 (960; 0.075)	1.63	566 (190; 0.067)	387 (140; 9070), 656 (210; 4980; 0.08)	548 (23.2), 588 (23.9), 635
F-2	291 (37.5), 323 (30.8), 354 (38.1), 419 (7.7), 439 (6.8)	591 (950; 0.047)	1.12	588 (570; 0.042)	475 (620; 5500; 0.16), 665 (680; 4820), 800 (480)	542(16.0), 586 (15.5),
F-3	288 (37.7), 339 (35.7), 355 (30.8), 443 (9.2), 463 (8.8), 529 (1.0)	593 (680; 0.073)	1.41	590 (510; 0.065)	400 (670; 11480), 635 (660; 3790; 0.11)	550 (14.0), 590 (14.2)
F-4	284 (48.2), 341 (31.9), 355 (30.9), 441 (10.3), 465 (9.2), 530 (1.2)	593(980; 0.076)	1.37	592 (758; 0.067)	400 (880; 11000), 645 (800; 1670; 0.24)	554 (14.0), 584 (14.5)
F-5	293 (80.4), 324 (79.6), 361 (126.0), 441 (24.4), 486 (24.6), 510 (22.3)	602[e] (890 (97%), 30 (3%)); 0.015)	1.94	607[f] (825 (94%), 20 (6%)); 0.008[g])	*h*	588 (16.0), 629 (14.7)

[a] Measured at room temperature. [b] In butyronitrile glassy solutions at 77 K. [c] At a concentration of 5×10^{-5} mol/L. [d] Self-quenching rate constant. [e] At a concentration of 5×10^{-6} mol/L. [f] At a concentration of 5×10^{-6} mol/L in acetone. [g] In acetone solution. [h] Too weak to be measured.

considerable ground-state absorption from 550 to 600 nm in **F-5**, it is reasonable to believe that the red-shift is induced by self-absorption of the emission. The reduced intensity and lifetime at high concentrations could be attributed to a combination of self-quenching, self-absorption of emission and inner filter effect. The self-quenching constant is higher for **F-5** than those for **F-1**−**F-4**, possibly because of the extended π-system that facilitates the formation of excimer. This notion could be partially supported by the biexponential decay of the emission for **F-5** (shown in Table 1), in which the minor component may arise from an excimer emission. For the $^1\pi,\pi^*$ emission at the UV region for **F-5**, it also exhibits significant intensity decrease when the concentration increases. This emission is completely quenched when the concentration reaches 5×10^{-5} mol/L or higher. Because of the intense absorption of **F-5** in this spectral region, the reduced emission intensity should be caused predominately by self-absorption of the emission, although the inner filter effect due to the intense absorption could also contribute.

With respect to the emission spectra shown in Figure 3 for **F-1**−**F-5**, it is obvious that replacing the chloride co-ligand by the acetylide co-ligand reduces the emitting state energy, which has been seen in many reports for platinum C^N^N or terpyridyl complexes,[1,3g,6d,7−9,20] and could be attributed to the π-donating ability of the acetylide ligand that would decrease the ^{3}MLCT state energy. However, it is noted that the emission energy for **F-2**, **F-3**, and **F-4** is quite similar, which probably reflects the admixture of ^{3}ILCT character that is independent of the nature of the co-ligand into the emitting state. The reduced emission energy of **F-2** compared to that of **F-1** is similar to that observed for the platinum C^N^N complexes without the fluorenyl substituent and could also be explained by the involvement of the ^{3}ILCT character into the emitting state.[9] Another point should be noticed is that the emission energies for all five complexes are quite similar to their respective platinum C^N^N congeners without the 4′-fluorenyl substituent.[6d,7,9] This feature is consistent with that observed from the UV−vis absorption

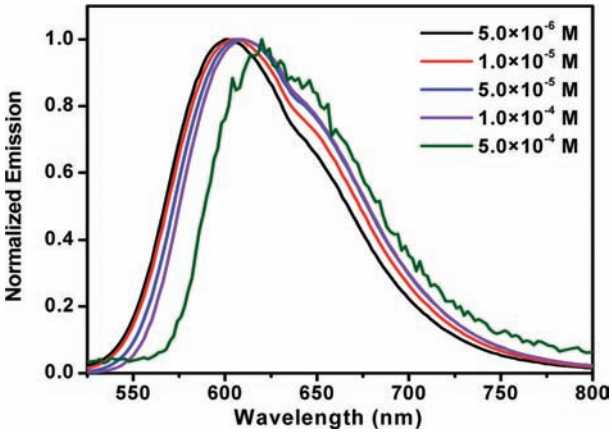

Figure 6. Normalized emission spectra of **F-5** at different concentrations in CH_2Cl_2 at room temperature. λ_{ex} = 441 nm.

study, and indicates that the fluorenyl substituent likely twists from the plane of the Pt(C^N^N) component. Consequently, electronic interaction between the fluorenyl substituent and the C^N^N ligand is reduced. However, introducing the fluorenyl substituent on the C^N^N ligand pronouncedly enhances the emission efficiency and increases the emission lifetime for these complexes compared to their respective Pt complexes without the fluorenyl substituent,[6d,9] which is testified by **F-1**, **F-2**, and **F-3**.

F-1−**F-4** are emissive in butyronitrile at 77 K. Compared to the emission at room temperature in CH_2Cl_2, the emission spectra shift to higher-energy and exhibit clear vibronic structures, as exemplified in Figure 7 for **F-1** and Supporting Information, Figure S5 for **F-3** and listed in Table 1 for the other three complexes. The vibronic progression is in the range of 930 cm^{-1} to 1390 cm^{-1} for these complexes, which falls into the skeletal stretching modes of the C^N^N ligand.[7] These spectral features are similar to those of C^N^N platinum acetylide complexes reported by Che.[1] The hypsochromic shift of the emission spectra at 77 K could be due to the rigidochromic effect, which is commonly seen in many

transition-metal complexes including platinum complexes.[23] The lifetimes of these complexes at 77 K are also comparable to those reported in the literature for other platinum C^N^N or terpyridyl complexes.[1,3g,6d,7−9] However, the thermally induced Stokes shift for **F-1** (580 cm^{-1}) and **F-5** (395 cm^{-1}) is much smaller than those for **F-2** (1440 cm^{-1}), **F-3** (1230 cm^{-1}), and **F-4** (1160 cm^{-1}). Considering the emission energy, the shape of the spectrum, the lifetime, and the thermally induced Stokes shift, we tentatively assign the emitting state at 77 K as ^{3}MLCT for **F-2**−**F-4**, and ^{3}MLCT/$^3\pi,\pi^*$ for **F-1** and **F-5**.

Transient Difference Absorption. The lifetimes measured from the decay of the emission of **F-1**− **F-5** suggest that the triplet excited state is much long-lived than the laser pulse width. Therefore, triplet excited-state absorption is expected to be observed for these complexes. Figure 8 displays the triplet transient difference absorption (TA) spectra of **F-1**−**F-4** in degassed CH_3CN solution at zero time-delay after the excitation. The time-resolved TA spectrum is exemplified in Figure 8 for **F-2** as well. The transient absorption from **F-5** is too weak to be detected. This is partially attributed to the very poor solubility of this complex in CH_3CN, which limits the highest concentration we could use for the TA experiment and prevents efficient population of the excited state because of the very dilute solution. On the other hand, the lack of observable TA from **F-5** could be hypothetically related to its lower triplet excited-state quantum yield, which is partially reflected by its significantly lower emission quantum yield compared to those for **F-1**−**F-4**.

F-1 and **F-2** exhibit broad positive absorption from 380 to 830 nm. The profiles of the TA spectra of **F-3** and **F-4** are similar to that of **F-1**, with the exception that some bleaching occurred in the region of 420−480 nm and a flatter and stronger absorption in the NIR region of 770−850 nm. The facts that the bleaching band position is consistent with the charge transfer band in the UV−vis absorption spectra and the different features in the NIR region indicate that the TA could possibly originate from the ^{3}MLCT/^{3}ILCT/^{3}LLCT state for **F-3** and **F-4**. For **F-1** and **F-2**, the excited-state that gives rise to the transient absorption could be ^{3}MLCT/^{3}ILCT. All the TA decays monoexponentially throughout the whole spectral range monitored, indicating that the transient absorption arises from the same excited state or excited states in close proximity that are in equilibrium. In addition, the lifetime measured from the decay of the transient absorption and from the decay of the emission are essentially consistent, suggesting that the TA might arise from the same excited state that emits, or a state that is in equilibrium with the emitting state. These pieces of evidence further support the aforementioned assignment for the TA of these complexes.

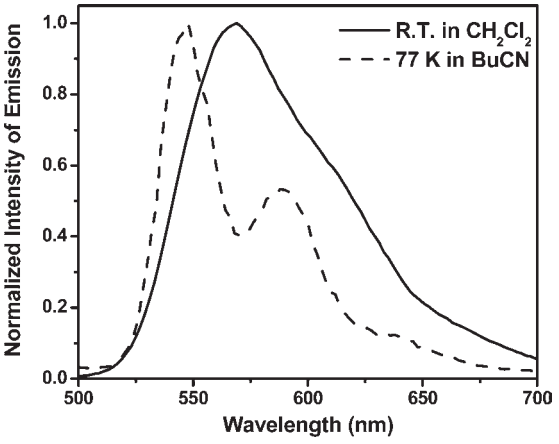

Figure 7. Emission spectra of **F-1** at room temperature and at 77 K. λ_{ex} = 423 nm. $c = 5 \times 10^{-5}$ mol/L.

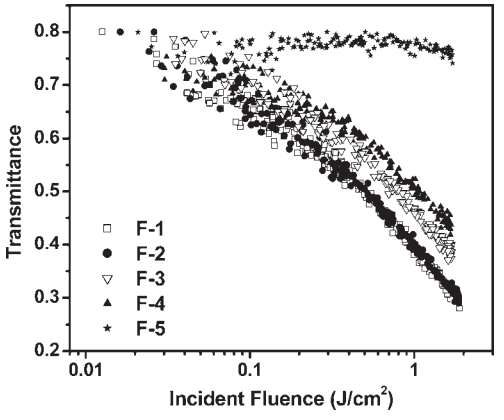

Figure 9. Transmittance vs incident fluence curves of **F-1**−**F-5** in CH_2Cl_2 for 4.1 ns laser pulses at 532 nm in a 2 mm cell. The linear transmission was adjusted to 80%.

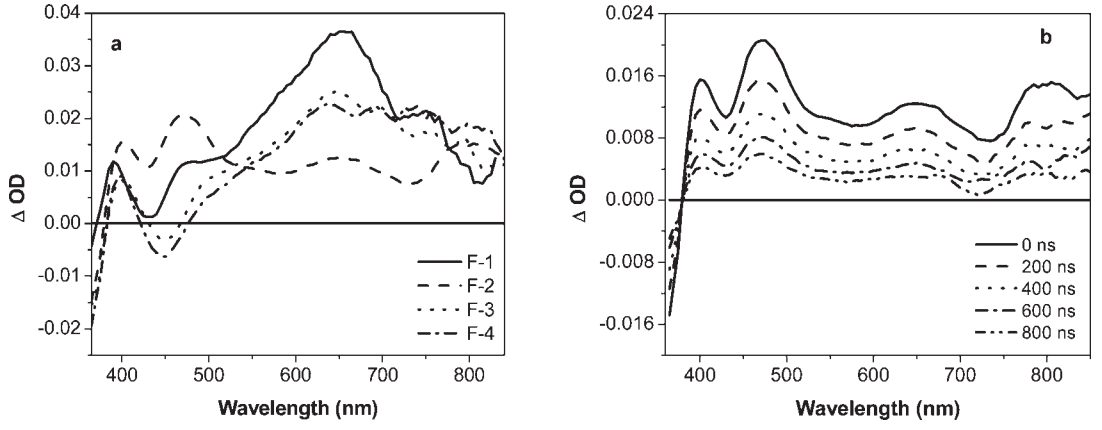

Figure 8. (a) Triplet transient difference absorption spectra of **F-1**−**F-4** in argon-degassed CH_3CN solution at room temperature at zero time delay following 355 nm excitation. (b) Time-resolved TA spectra for **F-2** in degassed CH_3CN solution.

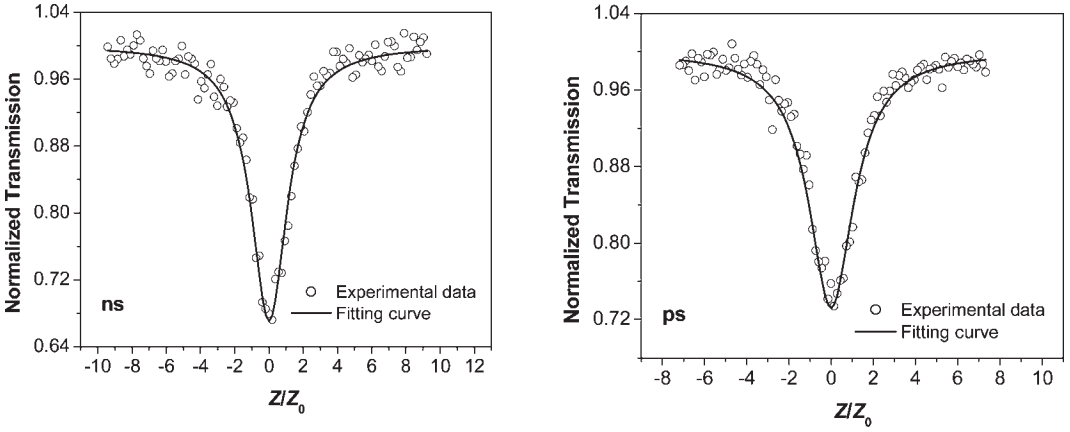

Figure 10. Nanosecond and picosecond open-aperture Z-scan experimental data and fitting curves for **F-1** at 532 nm. The energy used was 3.9 μJ for ns Z scan and 1.5 μJ for ps Z scan, and the beam radius at the focal point was 30 μm for ns Z scan and 34 μm for ps Z scan.

Table 2. Excited-State Absorption Cross Sections of **F-1**−**F-4** in CH_2Cl_2 at 532 nm

	$\sigma_0{}^a$ (10^{-18} cm^2)	$\sigma_S{}^b$ (10^{-18} cm^2)	$\sigma_T{}^c$ (10^{-18} cm^2)	σ_S/σ_0	σ_T/σ_0	$\Phi\sigma_T/\sigma_0$
F-1	0.765	62 ± 2	245 ± 5	81	320	25.6
F-2	0.536	80 ± 3	103 ± 3	149	192	30.8
F-3	3.29	130 ± 5	145 ± 5	40	44	4.8
F-4	4.21	100 ± 5	75 ± 5	24	18	4.3
(C^N^N)PtC$_5$H$_7$	1.60	19 ± 1	46 ± 2	12	29	14.7

[a] Ground-state absorption cross-section. [b] Singlet excited-state absorption cross-section. [c] Triplet excited-state absorption cross-section.

Reverse Saturable Absorption and Z-Scan Measurements. As discussed in the TA section, complexes **F-1**− **F-4** exhibit broad positive TA in most of the visible to the near-IR region, which implies that their excited-state absorption cross-sections are larger than the ground-state absorption cross-sections. In addition, the TA decay times are hundreds of nanoseconds. Therefore, reverse saturable absorption (RSA) could occur for these platinum complexes under the irradiation of ns laser pulses. To demonstrate this, the nonlinear transmission experiments were carried out for **F-1**−**F-5** in CH_2Cl_2, and the results are illustrated in Figure 9.

When the incident fluence is increased, the transmittance of **F-1**−**F-4** decreases significantly. The RSA threshold, defined as the incident fluence at which the transmittance decreases to 70% of the linear transmittance, is 0.29 J/cm^2 for **F-1** and **F-2**, 0.48 J/cm^2 for **F-3**, and 0.65 J/cm^2 for **F-4**. When the incident fluence is increased to 1.8 J/cm^2, the transmittance drops to 0.28 for **F-1** and **F-2**, 0.37 for **F-3**, and 0.42 for **F-4**. For **F-5**, the transmittance almost keeps constant even at high fluences, indicating that almost no RSA occurs, which is consistent with the TA results discussed in the previous section. The strength of the RSA for these five complexes obviously follows this trend **F-1** = **F-2** > **F-3** > **F-4** > **F-5**.

According to our previous studies, one of the key parameters that determines the degree of RSA is the ratio of the excited-state absorption cross-section to that of the ground-state. The ground-state absorption cross-sections at 532 nm for these complexes are 7.7×10^{-19} cm^2 for **F-1**, 5.4×10^{-19} cm^2 for **F-2**, 3.3×10^{-18} cm^2 for **F-3**, and 4.2×10^{-18} cm^2 for **F-4** by using the ε values obtained from their UV−vis absorption spectra and the conversion equation $\sigma = 2303\varepsilon/N_A$, where N_A is the Avogadro constant. To obtain the excited-state absorption cross-sections, open-aperture Z-scan[24] experiments that measure the transmission changes due to nonlinear absorption were carried out at 532 nm using both ns and ps laser pulses for **F-1**−**F-4**. Fitting of these ns and ps open-aperture Z-scan experimental data using the 5-band model will allow us to extract both the singlet and triplet excited-state absorption cross-section.[19]

Figure 10 shows the open-aperture Z-scan experimental data and the fitting curves for **F-1**. **F-2**−**F-4** exhibit the similar results, while **F-5** shows negligible nonlinear absorption. The transmission for **F-1**−**F-4** decreases when the samples are moved close to the focal plane, that is, the incident fluence increases, indicating the occurrence of reverse saturable absorption. By applying the ground-state absorption cross-sections determined from the UV−vis absorption, the triplet and singlet excited-state lifetimes obtained from the decay of the respective ns and fs transient absorption (the τ_T's are listed in Table 1, the τ_S is 12.1 ps for **F-1**, 6.9 ps for **F-2**, and 5.3 ps for **F-3** and **F-4**), and the triplet excited-state quantum yields (listed in Table 1) to the five-band model, and using the procedure described previously,[19] we obtained a single pair of excited-state absorption cross-section values (σ_s, σ_T) that simultaneously fit both the nanosecond and picosecond Z scans. These results are compiled in Table 2. For comparison purpose, Z scans of the corresponding (C^N^N)PtC$_5$H$_7$ complex[6d] has also been carried out, and the fitting results are listed in Table 2.

(23) (a) Kunkely, H.; Vogler, A. *J. Am. Chem. Soc.* **1990**, *112*, 5625. (b) Wan, K.-T.; Che, C.-M.; Cho, K.-C. *J. Chem. Soc., Dalton Trans.* **1991**, 1077. (c) Hissler, M.; Connick, W. B.; Geiger, D. K.; McGarrah, J. E.; Lipa, D.; Lachicotte, R. J.; Eisenberg, R. *Inorg. Chem.* **2000**, *39*, 447. (d) Lai, S.-W.; Chan, M. C.-W.; Cheung, T.-C.; Peng, S.-M.; Che, C.-M. *Inorg. Chem.* **1999**, *38*, 4046.

(24) Sheik-Bahae, M.; Said, A. A.; Wei, T.-H.; Hagen, D. J.; Stryland, E. W. V. *IEEE J. Quantum Electron.* **1990**, *26*, 760.

It is obvious that the excited-state absorption cross-section values (both σ_s and σ_T) at 532 nm for **F-1**−**F-4** are much larger than those for the (C^N^N)PtC_5H_7 complex, which is in line with the trend observed in the UV−vis absorption, reflecting the influence of fluorenyl unit on the C^N^N complexes. The ratios of σ_S/σ_0 and σ_T/σ_0 for **F-1** and **F-2** are among the largest values reported in the literature.[6g,25] When fitting the Z-scan results, the population fraction on related excited states are calculated versus time. The results are exemplified in Supporting Information, Figure S6 for **F-1**. It is apparent that for ns excitation, the triplet excited states (T_1 and T_2) are much more populated than the singlet excited states (S_1 and S_2). Therefore, the excited-state absorption for ns laser pulses is dominated by the triplet excited-state absorption. In such a case, the RSA is not only predominantly determined by the ratio of σ_T/σ_0, but also affected by the triplet excited-state quantum yield. Taking these factors into account, we found that the ratio of $\Phi\sigma_T/\sigma_0$ (listed in Table 2) correlates very well with the observed RSA trend shown in Figure 9. Therefore, to improve the RSA for ns laser pulses, improving the ratio of $\Phi\sigma_T/\sigma_0$ is crucial. In the case of complexes having similar excited-state absorption cross-section, the complex with the minimum ground-state absorption cross-section and higher triplet quantum yield would give rise to a larger ratio of $\Phi\sigma_T/\sigma_0$ and thus stronger RSA.

Conclusion

Mononuclear and dinuclear platinum(II) 6-phenyl-4-(9,9-dihexylfluoren-2-yl)-2,2′-bipyridine complexes **F-1**−**F-5** were synthesized, and their photophysics were systematically investigated. Because of the electron-donating ability of the fluorenyl substituent, the lowest-energy singlet and triplet excited states possess intraligand charge transfer character, possibly mixed with some ^{3}MLCT character. **F-1**−**F-4** exhibit broad triplet transient difference absorption in the visible to the near-IR region; therefore, they give rise to a strong reverse saturable absorption for ns laser pulses at 532 nm. The degree of reverse saturable absorption follows this trend: **F-1** = **F-2** > **F-3** > **F-4** > **F-5**, which is mainly determined by the ratio of the triplet excited-state absorption cross-section to that of the ground-state and the triplet excited-state quantum yield. Introducing the fluorenyl substituent on the C^N^N ligand causes a pronounced effect on the photophysics of these complexes, which is reflected by their much larger molar extinction coefficients for their low-energy charge transfer absorption band, longer triplet excited-state lifetimes, higher emission quantum yields, and significantly increased ratios of the excited-state absorption cross-section to that of the ground-state compared to those of their corresponding Pt complexes without the fluorenyl substituent. Additionally, **F-2** shows much improved solubility in CH_2Cl_2 (∼150 mg/mL), making it possible to prepare high-concentration solutions for two-photon absorption study in the near-IR region. Therefore, two-photon induced excited-state absorption was observed in the near-IR region for this complex. These results will be reported later.

Acknowledgment. Financial support from the National Science Foundation (CAREER CHE-0449598) and the Army Research Laboratory (W911NF-06-2-0032) is greatly appreciated. We are grateful to Dr. Joy E. Haley at the UES Inc. and the Air Force Research Laboratory for measuring the singlet excited-state lifetime and to Zhongjing Li at Sun's group at NDSU for measuring the fluorescence spectra of the related ligands and fluorene.

Supporting Information Available: Comparison of the UV−vis absorption spectra of **F-1**−**F-3** to their respective platinum C^N^N complexes without the fluorenyl substituent, the excitation spectra of **F-5** in CH_2Cl_2, the fluorescence spectra of ligand **5**, 2,7-diethynyl-9,9-dihexylfluorene, and fluorenes in CH_2Cl_2, the normalized emission spectra of **F-4** at different concentrations at room temperature, the emission spectra of **F-3** in CH_2Cl_2 at room temperature and in butyronitrile at 77 K, and the population fraction versus time on different excited states for **F-1** upon ns laser excitation. This material is available free of charge via the Internet at http://pubs.acs.org.

(25) Pritchett, T. M.; Sun, W.; Zhang, B.; Ferry, M. J.; Li, Y.; Haley, J. E.; Machie, D. M.; Shensky, W., III; Mott, A. G. *Opt. Lett.* **2010** (in press).